

Fundamental study for application of 3D phase-sensitive inversion recovery sequence to multiple sclerosis

3D phase-sensitive inversion recovery を多発性硬化症に応用するための基礎的検討

ENOKI Takuya^{1, 2)}, JOMOTO Wataru²⁾, KIDA Katsuhiko¹⁾, GOTO Sachiko¹⁾, KOTOURA Noriko²⁾

1) Graduate School of Health Sciences, Okayama University

2) Department of Radiological Technology, Hyogo Medical University Hospital

Key words: Phase sensitive inversion recovery, Inversion time, Magnetic resonance imaging, Brain

[Abstract]

This study clarified the relationship between imaging parameters and contrast during application of the 3D phase-sensitive inversion recovery (PSIR) method for detection of multiple sclerosis. In this phantom study, we investigated the effects of the turbo field echo (TFE) factor, shot interval, and inversion time (TI) on contrast. A TFE factor of 30 and shot interval of 1000 ms were employed. In the in vivo study, visual evaluations were performed to assess the brain tissue contrast when TI variations were noted. This in vivo study enrolled 10 healthy volunteers. 3D-PSIR images were acquired with six different inversion times (300, 400, 500, 600, 700, and 800 ms). A longer inversion time for 3D-PSIR increased the contrast of the brain tissue. To apply 3D-PSIR to multiple sclerosis lesions, a TI of 700 ms is suitable when the TFE factor is 30 and the shot interval is 1000 ms.

【要旨】

本研究の目的は、3D PSIRを多発性硬化症へ応用するために、撮像パラメーターと脳組織コントラストの関係を明らかにすることである。ファントム実験で、TFE factor, shot interval, TIがコントラストに与える影響を検討した。TFE factorは30, shot intervalは1000 msが採用された。健康ボランティアでTI (300–800 ms) を変化させ、脳組織コントラストについて視覚評価を行った。TIを長くするとコントラストは向上した。3D-PSIRを多発性硬化症へ応用するには、TFE factorが30, shot intervalが1000 msの場合、TIは700 msが最適である。

1 Introduction

Double inversion recovery (DIR) has been widely used to detect cortical lesions in patients diagnosed with multiple sclerosis (MS)^{1–4)}. However, DIR has been reported to have a low signal-to-noise ratio (SNR) and sensitivity for cortical lesions⁴⁾. Phase-sensitive inversion recovery (PSIR) is a T₁-weighted sequence that uses the inversion recovery (IR) method, which has been reported to improve the detection of cortical lesions in patients with MS, compared to that of DIR, because of its excellent contrast between the white matter

(WM), gray matter (GM), and cerebrospinal fluid (CSF) and higher SNR^{5–11)}.

In a previous study, PSIR was obtained by reconstructing real images acquired using a 2D-IR turbo spin-echo (TSE) sequence^{5–11)}. In the present study, we investigated the contrast of 3D-PSIR based on a gradient echo sequence, in which two signals were acquired and phase correction was performed. Since 3D-PSIR can prevent IR-induced signal polarity reversal by phase correction, it is a well-known imaging sequence that enables visualization of the injured myocardium regardless of the inversion time (TI) to nullify the signal intensity of the normal myocardium in late gadolinium-enhanced cardiac imaging¹²⁾. However, because PSIR uses the IR method, the contrast is expected to change depending on the timing of signal acquisition^{7, 13)}. In a previous study, a TI of approximately 400 ms was used in 2D-PSIR^{5–11)}; however,

榎 卓也^{1, 2)}, 城本 航²⁾, 木田 勝博¹⁾, 後藤 佐知子¹⁾, 琴浦 規子²⁾

1) 岡山大学大学院保健学研究科

2) 兵庫医科大学病院 放射線技術部

Received July 31, 2022; accepted January 3, 2023

because the repetition time (TR) and echo time (TE) are different in each report, the contrast is expected to differ with the same TI. Furthermore, the optimal TI may differ when using 3D-PSIR, and the turbo field echo (TFE) factor and shot interval are also expected to affect the contrast.

The purpose of this study was to clarify the relationship between imaging parameters and contrast when applying the 3D-PSIR method for detection of MS.

2 Materials and Methods

2.1 Theory

Magnetic resonance imaging (MRI) scans were acquired using a 3.0-T MRI system with a 32-channel phased-array head coil (Ingenia; Philips Healthcare, Best, Netherlands). In the PSIR of this study, after the nonselective inversion pulse, signal acquisition was performed with a fast gradient echo after each of the two TIs. The first TI (first acquisition) acquired the magnitude- T_1 contrast image, and the second TI (second acquisition) acquired the reference image. Since the T_1 contrast image has an inverted signal polarity depending on the TI setting, the following procedure was used to calculate the PSIR image with preserved signal polarity: A B1 field correction map was created from the phase information obtained in the second acquisition, and phase correction was performed on the signals obtained in the first and second acquisitions. The phase-corrected signal was divided into real and imaginary parts using quadrature phase-sensitive detection, and the real and imaginary images were calculated using a complex Fourier transform. Subsequently, a magnitude image was calculated from the first acquisition and a phase image was calculated from the second acquisition. The magnitude image was multiplied by the phase image to reconstruct the real image and obtain the PSIR image. The

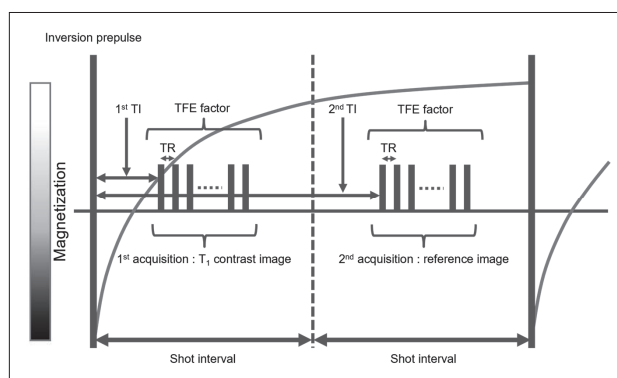


Fig.1 Overview of PSIR sequence

After TI from the inversion pulse, the T_1 contrast image was acquired by a fast gradient echo. After a certain time, a fast gradient echo was used to acquire a reference image. The PSIR was reconstructed from the two images, and the timing of the two image acquisitions was adjusted by the shot interval.

timing of the two acquisitions can be adjusted using shot intervals. Figure 1 presents an overview of the sequence.

2.2 Phantom study

To evaluate the image quality, we diluted manganese chloride tetrahydrate (MCT) and agar with saline to create phantoms for the WM model (MCT 16 w/v%, agar 0.2 w/v%), GM model (8 w/v%, agar 0.3 w/v%), and CSF model (saline). The three phantoms were stored in a polypropylene case, which was filled with agar diluted with saline (0.1 w/v%). Figure 2 shows an overview of the phantom. T_1 and T_2 values of these materials are listed in Table 1. Image quality was evaluated by the contrast-to-noise ratio (CNR) using a region of interest (ROI) for each phantom (Fig.3). The signal intensity was measured on the console and the CNR was calculated using the following formula:

$$\text{CNR} = \frac{|SI_a - SI_b|}{SD_{BG}}, \quad (1)$$

where SI_a and SI_b are the mean signal intensities in phantoms a and b, respectively; SD_{BG} is the standard deviation of the background signal intensity. The background ROI was elliptical and large to reduce variation

Table 1 T₁ and T₂ values of materials

Material	T ₁ relaxation time (ms)	T ₂ relaxation time (ms)
WM model	824.0	67.6
GM model	1329.0	114.1
CSF model	2906.2	2047.0

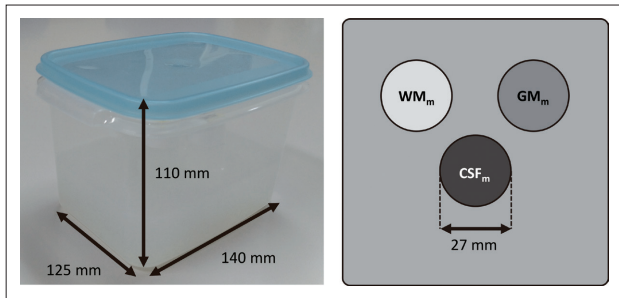


Fig.2 Overview of the phantom

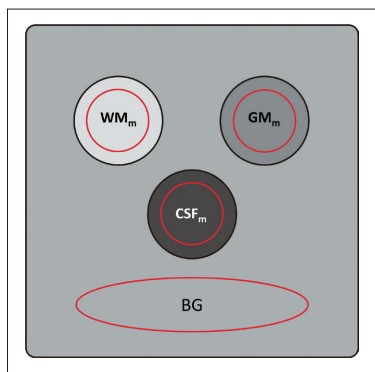


Fig.3 Example of region of interest setting

with measurement location. Preliminary experiments confirmed that the phantom created in this study provided a contrast similar to that of the *in vivo* phantom. Although it is desirable to create a phantom that simulates an MS lesion, the relaxation time of the lesion has not been clarified; therefore, it was difficult to create a phantom. In previous studies, MS lesions were more hypointense than GM lesions on 2D-PSIR⁵⁻¹¹⁾ and were expected to have a signal intensity between those of GM and CSF.

3D-PSIR was performed using a 3D TFE sequence. 3D-PSIR images with three different TFE factors (20, 30, and 40), four different shot intervals (800, 1000, 1200, and 1400 ms), and nine different TIs (160, 200, 300, 400, 500,

600, 700, 800, and 840 ms) were acquired to investigate the CNR. Other parameters were as follows: field of view, 250 mm; slice orientation, coronal; pixel size, 0.98 × 0.96 mm; slice thickness, 4 mm; number of slices, 6; number of excitations, 1; sensitivity encoding factor, 1; profile order, linear; TR, 10 ms; TE, 4.6 ms; flip angle (FA), 20°; PSIR FA, 5°; bandwidth (BW), 540 Hz/pixel; and scan time, 29 s–1 min 38 s.

2.2.1 Investigation of TFE factor

The shot interval and TI were fixed at 1000 ms and 600 ms, respectively, and the TFE factor varied between 20, 30, and 40. We measured the CNR between the WM model and GM models (WM_m-GM_m), WM model and CSF models (WM_m-CSF_m), and GM model and CSF models (GM_m-CSF_m) and evaluated the change in CNR with changes in the TFE factor.

2.2.2 Investigation of shot interval

The TFE factor and TI were fixed at 30 and 600 ms, respectively, and the shot interval varied between 800, 1000, 1200, and 1400 ms. We measured the CNR between WM_m-GM_m, WM_m-CSF_m, and GM_m-CSF_m and evaluated the change in CNR with the changes in the shot interval.

2.2.3 Investigation of TI

The TFE factor and shot interval were fixed at 30 and 1000 ms, respectively, and TI varied between 160, 200, 300, 400, 500, 600, 700, 800, and 840 ms. We measured the CNR between WM_m-GM_m, WM_m-CSF_m, and GM_m-CSF_m and evaluated the change in CNR with the changes in TI. We evaluated the changes in the mean signal intensities of each phantom associated with TI change.

2.3 In vivo study

Ten healthy volunteers (five males and five females; age range, 23–57 years; median [interquartile range] age, 39.5 [12.5] years) were

enrolled in this study. The Institutional Review Board of Hyogo Medical University approved this study, and informed consent was obtained from all participants in accordance with the Declaration of Helsinki (approval number 202104-521).

3D-PSIR was performed using a 3D TFE sequence. 3D-PSIR images with six different TIs (300, 400, 500, 600, 700, and 800 ms) were acquired to investigate the brain tissue contrast. Other parameters were as follows: field of view, 230 mm; slice orientation, transverse; pixel size, 0.85×0.85 mm; slice thickness, 3 mm; number of slices, 35; number of excitations, 1; sensitivity encoding factor, 2; profile order, linear; TFE factor, 30; shot interval, 1000 ms; TR, 10 ms; TE, 4.6 ms; FA, 20° ; PSIR FA, 5° ; BW, 540 Hz/pixel; and scan time, 2 min 17 s. The imaging slab was parallel to the anterior commissure-posterior commissure line, and the center of the imaging slab was set at the level of the insular cortex.

2.3.1 Visual evaluation

Five radiologists (10–26 years of reading experience) performed the visual evaluation using the normalized ranking method¹⁴. WM-GM, WM-CSF, and GM-CSF contrasts at the insular cortex level were evaluated. The medical imaging display monitor was set to a six-split display, and the six TI images were randomly placed for each evaluation item and for each volunteer, and ranked accordingly. Since 3D-PSIR has a different background signal, the image was magnified to the furthest extent, so that

the background signal was not observed.

2.3.2 Statistical analysis

Kendall's coefficient of concordance (W) was calculated from the ranked results obtained from the visual evaluation. W ranges from 0 to 1, where 0 indicates no agreement among raters and 1 indicates complete agreement. The ranked results were normalized, and a one-way analysis of variance was performed on the means of the normalized scores. The modified least significant difference (MLSD) of the Fisher–Hayter procedure was used to determine significant differences among the ranks¹⁵.

Statistical analysis was performed using the JMP Pro ver.15.2.0 software (SAS Institute, Cary, NC, USA). Statistical significance was set at $p < 0.05$.

3 Results

3.1 Phantom study

Figures 4 and 5a show MR images and

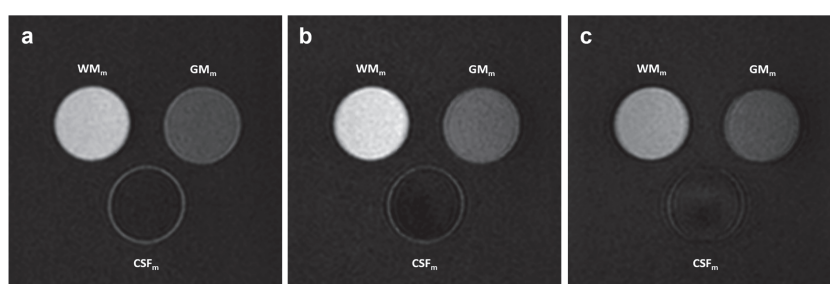


Fig.4 MR images for different TFE factor
(a) TFE factor=20. (b) TFE factor=30. (c) TFE factor=40.

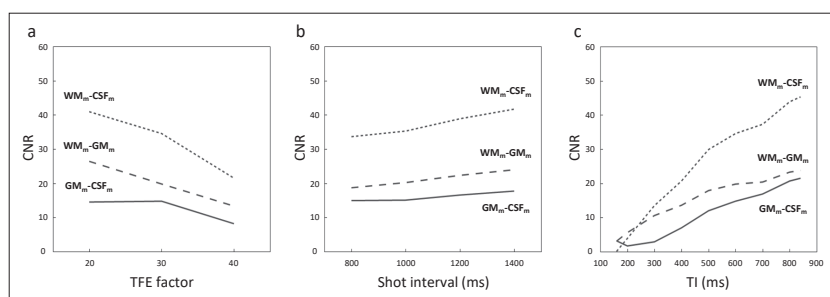


Fig.5 Relationship between CNR of the phantom and each parameter
(a) CNR of WM_m-CSF_m, WM_m-GM_m, and GM_m-CSF_m for different TFE factors.
(b) CNR of WM_m-CSF_m, WM_m-GM_m, and GM_m-CSF_m for different shot intervals.
(c) CNR of WM_m-CSF_m, WM_m-GM_m, and GM_m-CSF_m for different TIs.

CNR results for the different TFE factors. The CNR decreased as the TFE factor increased. When the TFE factor was 40, strong blurring occurred. The CNR increased as the shot interval and TI increased (Fig.5b and c). The signal intensities of WM_m, GM_m, and CSF_m increased as TI increased. The signal intensities of each phantom increased as TI increased, and the difference in the signal intensities of each phantom became larger (Fig.6).

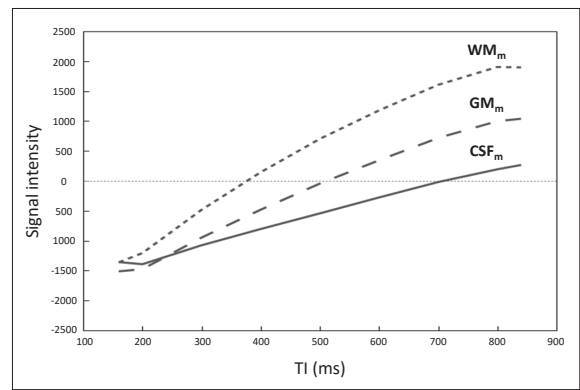


Fig.6 Relationship between signal intensity of the phantom and each TI

3.2 In vivo study

Figure 7 shows MR images of a volunteer. The tissue contrast varied for each TI. The signal intensities of WM, GM, and CSF increased as TI increased.

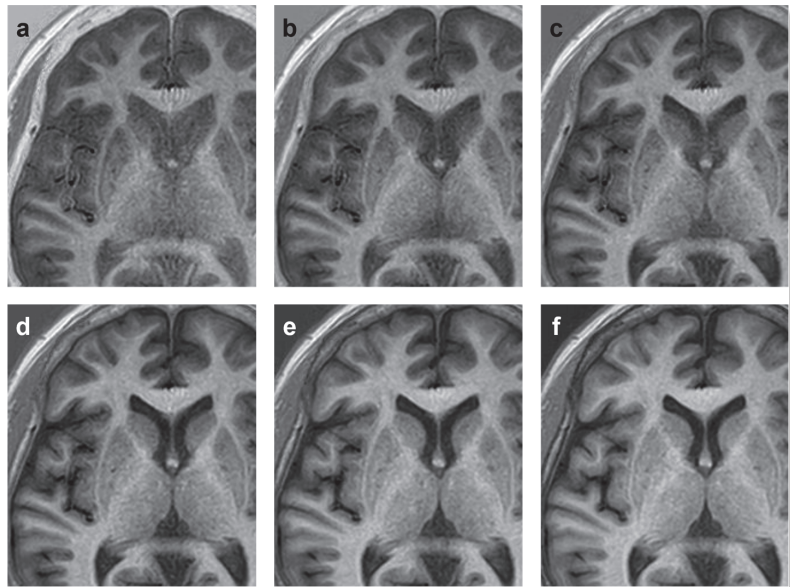


Fig.7 Example of a PSIR image with the TI varying from 300 ms to 800 ms

(a) TI=300 ms. (b) TI=400 ms. (c) TI=500 ms. (d) TI=600 ms. (e) TI=700 ms. (f) TI=800 ms.

The rank order of the visual evaluation of the WM-GM contrast was 600 > 700 > 500 > 800 > 400 > 300 (Table 2). The differences in the normal scores among these ranks were 0.323, 0.212, 0.350, 0.359, and 0.628, respectively, and there were no significant differences between 500 and 700 ($W = 0.55$, $p < 0.001$, $MLSD = 0.306$). The rank order of the visual evaluation for WM-CSF contrast was 700 > 800 > 600

Table 2 Results of visual evaluation in WM-GM and significant differences in normal scores between each rank using Fisher-Hayter procedure (MLSD = 0.306)

Rank	TI (ms)	TI (ms)					
		600	700	500	800	400	300
1	600	0	0.323 *	0.535 *	0.885 *	1.245 *	1.873 *
2	700		0	0.212 <i>n.s.</i>	0.562 *	0.921 *	1.550 *
3	500			0	0.350 *	0.709 *	1.338 *
4	800				0	0.359 *	0.987 *
5	400					0	0.628 *
6	300						0

Significant difference: the difference between each rank is larger than that of the MLSD ($\alpha = 0.05$) and indicated with *. MLSD, modified least significant difference; *n.s.*, not significant; TI, inversion time

Table 3 Results of visual evaluation in WM-CSF and significant differences in normal scores between each rank using Fisher-Hayter procedure (MLSD = 0.168)

Rank	TI (ms)	TI (ms)										
		700	800	600	500	400	300					
1	700	0	0.057	<i>n.s.</i>	0.321	*	1.008	*	1.464	*	2.094	*
2	800		0		0.264	*	0.951	*	1.407	*	2.037	*
3	600				0		0.687	*	1.143	*	1.773	*
4	500						0		0.456	*	1.086	*
5	400								0		0.630	*
6	300										0	

Significant difference: the difference between each rank is larger than that of the MLSD ($\alpha = 0.05$) and indicated with *. MLSD, modified least significant difference; *n.s.*, not significant; TI, inversion time

Table 4 Results of visual evaluation in GM-CSF and significant differences in normal scores between each rank using Fisher-Hayter procedure (MLSD = 0.183)

Rank	TI (ms)	TI (ms)										
		700	800	600	500	400	300					
1	700	0	0.148	<i>n.s.</i>	0.229	*	0.977	*	1.458	*	2.071	*
2	800		0		0.081	<i>n.s.</i>	0.829	*	1.310	*	1.923	*
3	600				0		0.748	*	1.228	*	1.842	*
4	500						0		0.480	*	1.094	*
5	400								0		0.614	*
6	300										0	

Significant difference: the difference between each rank is larger than that of the MLSD ($\alpha = 0.05$) and indicated with *. MLSD, modified least significant difference; *n.s.*, not significant; TI, inversion time

> 500 > 400 > 300 (Table 3). The differences in the normal scores among these ranks were 0.057, 0.264, 0.687, 0.456, and 0.630, respectively, and there were no significant differences between 700 and 800 ($W = 0.89$, $p < 0.001$, MLSD = 0.168). The rank order of visual evaluation for GM-CSF contrast was 700 > 800 > 600 > 500 > 400 > 300 (Table 4). The differences in the normal scores among these ranks were 0.148, 0.081, 0.748, 0.480, and 0.614, respectively. There were no significant differences between 700 and 800 or 800 and 600 ($W = 0.87$, $p < 0.001$, MLSD = 0.183).

4 Discussion

We conducted a fundamental study of imaging parameters for the application of 3D-PSIR in the detection of MS. The contrast between GM and CSF was important because MS lesions were expected to have a signal

intensity between those of GM and CSF⁵⁻¹¹. However, because MS lesions are located not only at the WM but also at the GM, evaluation of WM-GM and WM-CSF contrasts was necessary. Our study clarified the relationship between WM, GM, and CSF contrasts and varying TFE factors, shot intervals, and TIs in 3D-PSIR.

The phantom study showed that the CNR increased with a lower TFE factor, longer shot interval, and longer TI. A high TFE factor caused blurring and a decrease in CNR owing to the large number of echoes to be recorded and the inclusion of echoes with low signal intensities. A longer shot interval and TI accelerated the recovery of the longitudinal magnetization; therefore, the CNR of each phantom increased. The TFE factor and shot interval significantly affected the scan time. Since the phantom study showed that the CNR of GM_m-CSF_m was maintained up to a TFE

factor of 30 and that the shot interval did not contribute significantly to CNR improvement, a TFE factor of 30 and shot interval of 1000 ms were employed. In the *in vivo* study, visual evaluations were performed to assess the contrast when TI variations were noted.

In the visual evaluation, considering the results of the phantom study, the WM-CSF and GM-CSF contrasts were expected to be the highest among the images with a TI of 800 ms; however, this was not the case. As TI increased, the signal intensity and contrast of each tissue increased. Nevertheless, we assumed that it was impossible to visually distinguish the contrast above a specific value. W values in the visual evaluation of WM-GM (0.55) were lower than those of WM-CSF and GM-CSF (0.89 and 0.87, respectively). Since the CNR of WM_m - GM_m was almost constant at a TI of 500–700 ms in the phantom study, we assumed that the inter-rater variance was increased in the visual evaluation of WM-GM. Based on the changes in the signal intensities of GM_m and CSF_m in the phantom study, a longer TI is expected to improve the contrast with the MS lesion. However, considering the results of the phantom study and visual evaluations, we assumed that a TI of 700 ms was appropriate.

A TI of approximately 400 ms was used in previous studies that utilized TSE^{5–11)} and was different from the optimal TI noted in this study, which utilized the gradient echo. Gradient echo-based 3D-PSIR imaging has been reported to improve the detection of spinal cord lesions in patients with MS with a TI of 350–400 ms^{16, 17)}. These reports also differ from our results, but this is owing to the differences in the target area. In the spinal cord, CSF is distributed around the WM, and the WM-CSF contrast is high, even with a relatively short TI. Therefore, we assumed that a TI of 350–400 ms is acceptable in the spinal cord region. These studies also used a TFE factor of 67–69, which was higher than

our imaging parameters of 30. A high TFE factor reduces the scan time but also causes a decrease in contrast and blurring; therefore, it must be considered carefully.

This study had some limitations. First, the TI setting is limited to a TFE factor of 30 and shot interval of 1000 ms. If other parameters are changed, the TI setting must be modified again. Secondly, a slice thickness of 3 mm was used. In a 3D sequence, it is desirable to use a slice thickness of approximately 1 mm. However, thicker slices were used to reduce the effect of noise because we focused on evaluating contrast. Third, the imaging parameters obtained in this study have not been evaluated in clinical use. Therefore, it is necessary to apply the results of the present study to the diagnosis of MS.

5 Conclusion

In 3D-PSIR, a smaller TFE factor, longer shot interval, and longer TI improve tissue contrast. To apply 3D-PSIR to MS lesions, a TI of 700 ms is suitable when the TFE factor is 30 and the shot interval is 1000 ms.

Declarations

Conflicts of Interest:

The authors declare that they have no conflicts of interest.

Ethical approval:

All procedures performed in this study involving human participants were in accordance with the ethical standards of the Institutional Review Board (IRB) and with the 1964 Helsinki declaration and its later amendments or comparable ethical standards.

Informed consent:

Informed consent was obtained from all individual participants included in the study.

表の説明

Table 1	試料の T_1 , T_2 値
Table 2	WM-GMの視覚評価の結果とFisher-Hayter法による各ランクの正規スコアの有意差 (MLSD=0.306)
Table 3	WM-CSFの視覚評価の結果とFisher-Hayter法による各ランクの正規スコアの有意差 (MLSD=0.168)
Table 4	GM-CSFの視覚評価の結果とFisher-Hayter法による各ランクの正規スコアの有意差 (MLSD=0.183)

図の説明

- Fig.1 PSIRシーケンスの概要
インバージョンパルスからTI後に高速グラジエントエコー法で T_1 コントラスト画像を取得する。一定時間後に再度高速グラジエントエコー法でリファレンス画像を取得する。2種類の画像からPSIR画像が再構成され、2種類の画像取得はshot intervalで調整できる。
- Fig.2 ファントムの概要
- Fig.3 ROI設定の例
- Fig.4 異なるTFEファクターのMR画像
(a) TFE factor=20. (b) TFE factor=30.
(c) TFE factor=40.
- Fig.5 各パラメーターとファントムCNRの関係
(a) 異なるTFEファクターで得られた WM_m - CSF_m , WM_m - GM_m , GM_m - CSF_m のCNR.
(b) 異なるshot intervalで得られた WM_m - CSF_m , WM_m - GM_m , GM_m - CSF_m のCNR.
(c) 異なるTIで得られた WM_m - CSF_m , WM_m - GM_m , GM_m - CSF_m のCNR.
- Fig.6 TIとファントム信号値の関係
- Fig.7 TIを300~800 msに変化させたときのPSIR画像の例
(a) TI=300 ms. (b) TI=400 ms. (c) TI=500 ms.
(d) TI=600 ms. (e) TI=700 ms. (f) TI=800 ms.

References

- Geurts JJ, et al.: Intracortical lesions in multiple sclerosis: improved detection with 3D double inversion-recovery MR imaging. *Radiology*, 236: 254-60, 2005.
- Calabrese M, et al.: Detection of cortical inflammatory lesions by double inversion recovery magnetic resonance imaging in patients with multiple sclerosis. *Arch Neurol*, 64: 1416-22, 2007.
- Calabrese M, et al.: A 3-year magnetic resonance imaging study of cortical lesions in relapse-onset multiple sclerosis. *Ann Neurol*, 67: 376-83, 2010.
- Seewann A, et al.: Postmortem verification of MS cortical lesion detection with 3D DIR. *Neurology*, 78: 302-8, 2012.
- Sethi V, et al.: Improved detection of cortical MS lesions with phase-sensitive inversion recovery MRI. *J Neurol Neurosurg Psychiatry*, 83: 877-82, 2012.
- Harel A, et al.: Phase-sensitive inversion-recovery MRI improves longitudinal cortical lesion detection in progressive MS. *PLoS One*, 11: e0152180, 2016.
- Hou P, et al.: Phase-sensitive T1 inversion recovery imaging: a time-efficient interleaved technique for improved tissue contrast in neuroimaging. *AJNR Am J Neuroradiol*, 26: 1432-8, 2005.
- Nelson F, et al.: Improved identification of intracortical lesions in multiple sclerosis with phasesensitive inversion recovery in combination with fast double inversion recovery MR imaging. *AJNR Am J Neuroradiol*, 28: 1645-9, 2007.
- Nelson F, et al.: Intracortical lesions by 3T magnetic resonance imaging and correlation with cognitive impairment in multiple sclerosis. *Mult Scler*, 17: 1122-9, 2011.
- Sethi V, et al.: MS cortical lesions on DIR: not quite what they seem? *PLoS One*, 8: e78879, 2013.
- Favaretto A, et al.: The parallel analysis of phase sensitive inversion recovery (PSIR) and double inversion recovery (DIR) images significantly improves the detection of cortical lesions in multiple sclerosis (MS) since clinical onset. *PLoS One*, 10: e0127805, 2015.
- Kellman P, et al.: Phase-sensitive inversion recovery for detecting myocardial infarction using gadolinium-delayed hyperenhancement. *Magn Reson Med*, 47: 372-83, 2002.
- Ishimori T, et al.: Preoperative identification of subthalamic nucleus for deep brain stimulation using three-dimensional phase sensitive inversion recovery technique. *Magn Reson Med Sci*, 6: 225-9, 2007.
- Harter HL: Expected values of normal order statistics. *Biometrika*, 48: 151-65, 1961.
- Williams LJ, et al.: Fisher's least significant difference (LSD) test. *Encyclopedia of Research Design*, 218: 840-53, 2010.
- Mirafzal S, et al.: 3D PSIR MRI at 3 Tesla improves detection of spinal cord lesions in multiple sclerosis. *J Neurol*, 267: 406-14, 2020.
- Fechner A, et al.: A 3T phase-sensitive inversion recovery MRI sequence improves detection of cervical spinal cord lesions and shows active lesions in patients with multiple sclerosis. *AJNR Am J Neuroradiol*, 40: 370-5, 2019.